Design and Evaluation of Hydroxamate Derivatives as Metal-Mediated Inhibitors of a Protein Tyrosine Kinase

Xianfeng Gu,[†,#] Yuehao Wang,[#] Anil Kumar,[†] Guofeng Ye,[†] Keykavous Parang,*[,†] and Gongqin Sun*[,#]

Department of Biomedical and Pharmaceutical Sciences and Department of Cell and Molecular Biology, University of Rhode Island, Kingston, Rhode Island 02881

Received September 5, 2006

Protein tyrosine kinases use two Mg^{2+} ions as cofactors in catalysis, one as the ATP−Mg complex (M1) and the other as an essential activator (M2). The M2-binding site has high affinity for transition metal cations such as cobalt and zinc. Taking advantage of this high affinity, we examined hydroxamates as metal-mediated inhibitors against C-terminal Src kinase (Csk), a protein tyrosine kinase. Of a small group of amino acid hydroxamates, tyrosine and phenylalanine hydroxamates inhibited Csk activity only in the presence of Co^{2+}. Four classes of phenylalanine and tyrosine hydroxamate derivatives were synthesized and evaluated as metal-mediated inhibitors of Csk, leading to improved inhibition and a better understanding of the structure−activity relationships. This study suggests that hydroxamates may serve as a general scaffold for developing metal-mediated inhibitors against protein tyrosine kinases. To the best of our knowledge, this is the first report of designing metal-mediated inhibitors against a protein tyrosine kinase by targeting a metal binding site.

Introduction

Protein tyrosine kinases (PTK) phosphorylate tyrosine hydroxyl groups in specific proteins.[1] They are essential components of signal transduction pathways that transmit extracellular signals to intracellular targets. PTKs can be transiently activated following signals for cell growth or differentiation.[1] Aberrant activation of specific PTKs is a key step in the initial transformation, angiogenesis, and metastasis for many types of cancers.[2,3] PTK inhibitor development has become a major approach for drug discovery.[4] Most current PTK inhibitors target the ATP-binding site. Although selective inhibitors competitive with ATP have been identified for specific protein kinases,[5,6] the discovery process is still labor-intensive because of the high structural homology between the ATP-binding site of protein kinases.[7] Therefore, identification of functionally critical binding sites and development of novel design strategies to target these sites are important for the long-term success of PTK inhibitors as successful drugs.

In addition to the Mg^{2+} (M1) bound to ATP to form the ATP−Mg complex as the phosphate donating substrate, a second Mg^{2+} (M2) is essential for PTK catalysis.[8−10] All other PTKs so far examined, including Src,[8,11] FGFR,[8] Yes,[9] v-Fps (a member of the Fps/Fes family),[12] IRK,[13] and EGFR,[14] also require M2 for activity. Crystal structure of IRK with catalytic ligands confirmed the presence of two Mg^{2+} ions in the active site.[15] The cAMP-dependent protein kinase (PKA), a Ser/Thr kinase, also binds to two Mg^{2+} in the active site, but the second Mg^{2+} is inhibitory by reducing its k_{cat}.[16] It appears likely that protein kinases require two Mg^{2+} ions for catalyzing the phosphorylation reaction.

Although Mg^{2+} is the physiological cofactor, Mn^{2+}, Co^{2+}, and Ni^{2+} can also substitute Mg^{2+} for binding to M2 to support PTK activity.[10] Furthermore, Mn^{2+}, Co^{2+}, and Ni^{2+} all have much higher affinity for the M2 binding site than Mg^{2+} does (K_d = 2.3 mM for Mg^{2+}, 12 μM for Mn^{2+}, 12 μM for Co^{2+}, and 20 μM for Ni^{2+}). Although Zn^{2+} could not serve as a Csk activator, it binds to the M2-binding site with a K_d of 0.65 μM, thus serving as a potent inhibitor competitive against M2.[10] The high affinity of Zn^{2+} for the Csk M2-binding site is exploited for a single-step affinity purification of GST-Csk from total bacterial extract on a Zn^{2+}-iminodiacetic acid agarose column.[17] The experiment demonstrates that Zn^{2+} could bind to the M2-binding site of Csk and iminodiacetic acid simultaneously. This result suggests that appropriate compounds can bind tightly to Csk by targeting M2.

Metal chelation and coordination are much stronger interactions than most of the weak interactions in biochemistry. Incorporating such interactions to inhibitor design is a well-established strategy.[18−23] Cisplatin, the most effective drug available today against several types of human cancers,[19,20] and hydroxamate-containing inhibitors against proteases[21−23] all take advantage of this tight binding. To the best of our knowledge, no metal-mediated inhibitor against PTKs has been reported so far.

We describe the evaluation of hydroxamate compounds as metal-mediated PTK inhibitors. We first identified tyrosine hydroxamate (TyrH) and phenylalanine hydroxamate (PheH) as potent metal-mediated inhibitors from screening a group of simple amino acid hydroxamates. A systematic effort was taken to determine the structure−activity relationships and optimize the inhibition. Four classes of PheH and TyrH derivatives were synthesized: (1) analogues with modified hydroxamate functional group (**5b**−**f**); (2) phenyl-substituted hydroxamate analogues (**17a**−**r**); (3) analogues with modified linker between hydroxamate and phenyl functional groups (**18u**,**v**); (4) TyrH analogues with modified α-amino group (−NH_2) (**23a**−**d**). These studies established a new family of PTK inhibitors.

Results and Discussion

Chemistry. Scheme 1 shows the solid-phase synthesis of tyrosine hydroxamate (**5a**) and thiohydroxamate (**5b**) in class I. Hydroxylamine Wang resin (**1**) was reacted with Fmoc-Tyr-

* To whom correspondence should be addressed. For K.P.: phone, 401-874-4471; fax, 401-874-5787; e-mail, kparang@uri.edu. For G.S.: phone, 401-874-5937; fax, 401-874-2202; e-mail, gsun@uri.edu, kparang@uri.edu.
[†] Department of Biomedical and Pharmaceutical Sciences.
[#] Department of Cell and Molecular Biology.

10.1021/jm061058c CCC: $33.50 © 2006 American Chemical Society
Published on Web 11/08/2006

Scheme 1. Solid-Phase Synthesis of Tyrosine Hydroxamate (**5a**) and Thiohydroxamate (**5b**)[a]

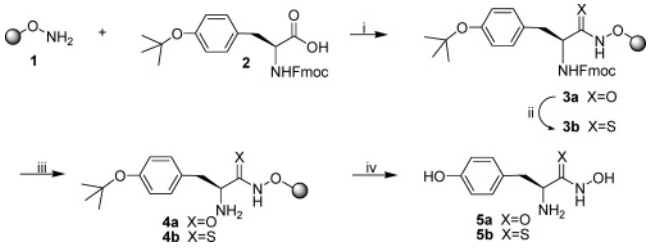

[a] Reagents: (i) HBTU, NMM/DMF (0.4 M); (ii) Lawesson's reagent, THF; (iii) piperidine in DMF (20%); (iv) TFA/CH_2Cl_2 (70%).

(^{t}Bu)-OH (**2**) in the presence of HBTU and *N*-methylmorpholine (NMM) to yield polymer-bound hydroxamate derivative (**3a**). The reaction between **3a** and 2,4-bis(4-methoxyphenyl)-[1,3,2,4]-dithiadiphosphetane 2,4-disulfide (Lawesson's reagent) in THF for 3 days afforded polymer-bound thiohydroxamate derivative **3b**. The deprotection of the Fmoc group in **3a** and **3b** with piperidine followed by treatment with TFA afforded **5a** and **5b**, respectively.

Scheme 2 displays the synthesis of *N*-methyl- and *N*-benzyltyrosine hydroxamates (**5c** and **5d**) in class I. Polymer-bound Fmoc protected methyl ester tyrosine (**8**) was synthesized from Wang resin (**6**) and Fmoc-Tyr(OH)-OMe using the Mitsunobu reaction in the presence of triphenylphosphine (PPh_3) and diisopropylazodicarboxylate (DIAD). The deprotection of Fmoc and methyl ester groups of **8** with NaOH (0.4 M) afforded polymer-bound tyrosine **9**. The subsequent reaction of **9** with the *N*-methyl- or *N*-benzylhydroxylamine hydrochloride in the presence of diisopropylcarbodiimide (DIC) and triethylamine (Et_3N) followed by cleavage using TFA afforded **5c** and **5d**, respectively.

Scheme 3 displays the syntheses of compounds **17a**−**r** and **18u**,**v** in classes II and III, respectively. The syntheses of polymer-bound compounds **13a**−**r** and **14s**,**t** were accomplished by the reaction between hydroxylamine Wang resin (**1**) and substituted Fmoc-Phe-OH derivatives (**11a**−**r** and **12s**,**t**) in the presence of HBTU. Deprotection of Fmoc group with piperidine followed by cleavage with TFA gave **17a**−**r** and **18u**,**v**, respectively.

Scheme 4 shows the procedure for the preparation of compounds **23a**−**d** in class IV. The hydroxyl groups in (*S*)-3-(4-hydroxylphenyl)propionic acid derivatives (**19a**−**d**) were protected by the acetyl group in the presence of acetic anhydride. Tyrosine acetylated compounds **20a**−**d** were reacted with hydroxylamine Wang resin (**1**) in the presence of HBTU to give **21a**−**d**. After removal of the Fmoc group in **21a** with piperidine (20%), the free amino group was reacted with benzyl bromide (BnBr) in pyridine to afford **21a′**. The deprotection of acetyl group in **21a′** and **21b**−**d** with sodium methoxide followed by cleavage with TFA/DCM (70%) afforded **23a**−**d**.

TyrH inhibits Csk Activity in a Co^{2+}-Dependent Manner. To explore the possibility of developing metal-mediated PTK inhibitors targeting the M2-binding site of Csk, a group of commercially available amino acid hydroxamates were evaluated. In the presence of 12 mM $MgCl_2$, none of the hydroxamates at 25 μM inhibited Csk more than 5% (Table 1). When 0.2 mM $CoCl_2$ in addition to 12 mM $MgCl_2$ was present, however, both TyrH and PheH inhibited Csk about 80%, while ArgH, LysH, LeuH, NorvalH, and GlyH also inhibited Csk, although to lesser extents. The addition of 0.2 mM Mn^{2+} or Ni^{2+} did not lead to hydroxamate inhibition of Csk.

The concentration-dependent inhibition of Csk by TyrH and PheH was then determined. TyrH up to 1 mM did not inhibit Csk in the absence of Co^{2+} but inhibited Csk with an IC_{50} of 9.5 μM in the presence of 0.2 mM Co^{2+} (Figure 1A). PheH exhibited similar Co^{2+}-dependent inhibition patterns with an IC_{50} of 15.5 μM (data not shown). As controls, the amino acid Tyr or Phe up to 1 mM did not inhibit Csk activity in the presence or absence of 0.2 mM $CoCl_2$. The requirement of both Co^{2+} and the hydroxamate group indicated that the inhibition was dependent on Co^{2+} binding to the hydroxamate group.

Two mechanisms could explain the Co^{2+} dependence of the inhibition. The first is based on Co^{2+} directly binding to Csk at the M2-binding site and on the inhibitors binding to Co^{2+}. An alternative explanation would be that Co^{2+} and the inhibitors formed some kind of complex(es), which inhibited Csk. This second mechanism would not depend on Co^{2+} directly binding to Csk. The results from two experiments strongly favored the first possibility. In the first experiment, the inhibition of Csk by 25 μM TyrH in the presence of 12 mM $MgCl_2$ and various concentrations of $CoCl_2$ was determined (Figure 1B). TyrH exhibited no inhibition in the absence of Co^{2+}. As the concentration of Co^{2+} increased, the level of inhibition by TyrH also increased, reaching about 80% at 0.2 mM Co^{2+}. The Co^{2+}-dependent inhibition by TyrH correlated to the binding of Co^{2+} to the M2 binding site predicted by the K_d (12 μM).

The second experiment compared the inhibition of Csk by 25 μM TyrH in the presence of different combinations of divalent metal cations (Figure 1C). On the basis of the affinities of metal cations for the M2 binding site, Co^{2+} occupies 90% of the M2-binding site in the presence of 12 mM Mg^{2+} and 0.2 mM Co^{2+} but only 20% of the M2-binding site in the presence of 2 mM Mn^{2+} and 0.2 mM Co^{2+}. If the inhibition of Csk by TyrH is dependent on Co^{2+} occupying the M2-binding site, much higher inhibition would be expected in the $Co^{2+}-Mg^{2+}$ combination. On the other hand, if Co^{2+} and TyrH formed inhibitory complex(es), the level of inhibition would be independent of which divalent metal cation occupies the M2-binding site. TyrH (25 μM) inhibited Csk about 80% in 12 mM Mg^{2+} and 0.2 mM Co^{2+} (condition b of Figure 1C) but only 13% in the presence of 2 mM Mn^{2+} and 0.2 mM Co^{2+} (condition e). In the presence of 12 mM $MgCl_2$ (condition a), 12 mM $MgCl_2$ + 2 mM $MnCl_2$ (condition c), and 2 mM $MnCl_2$ (condition d), 25 mM TyrH did not inhibit Csk. These results indicated that TyrH inhibition of Csk required Co^{2+} occupying the M2-binding site and argued for the interpretation that TyrH inhibited Csk as a metal-mediated inhibitor.

The inhibition of Csk by TyrH was noncompetitive against ATP (data not shown), suggesting that TyrH did not interfere with the binding of ATP-M1. When poly-E_4Y was the variable peptide substrate, the inhibition was mixed but leaning toward competitive with a K_i of 2 μM, determined by the Dixon plot ($1/v$ versus [I]). The near competitiveness with poly-E_4Y suggested that TyrH binding site was close to or partially overlapped with the peptide-binding site. TyrH also inhibited Src and FGFR in a Co^{2+}-dependent manner (K_i = 18 μM for Src; K_i = 23 μM for FGFR in the presence of 12 mM $MgCl_2$ and 0.2 mM $CoCl_2$). These results suggested that hydroxamate compounds could potentially be used as a general scaffold for developing metal-mediated inhibitors against various PTKs.

In order to further explore the structural requirements for designing metal-mediated inhibitors against PTKs, four classes of tyrosine and phenylalanine hydroxamate derivatives were synthesized and evaluated for their potency to inhibit Csk in the presence of cobalt:

I. Analogues with Modified Hydroxamate Functional Group. To understand the mechanisms of this metal-mediated

Scheme 2. Synthesis of *N*-Methyl- and *N*-Benzyltyrosine Hydroxamates (**5c** and **5d**)[a]

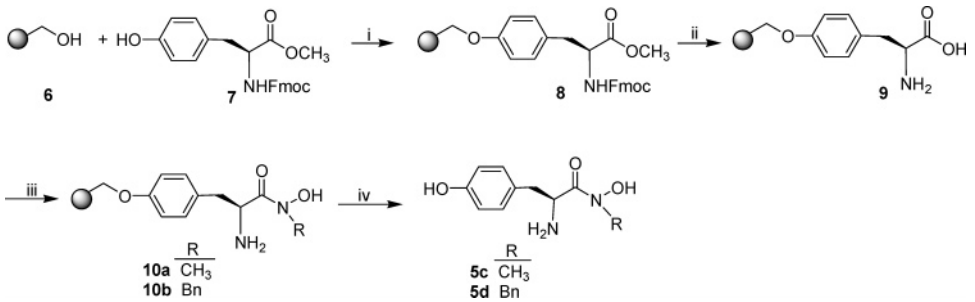

[a] Reagents: (i) DIAD, Ph_3P, CH_2Cl_2; (ii) NaOH (0.4 M); (iii) *N*-methylhydroxylamine hydrochloride or *N*-benzylhydroxylamine hydrochloride, DIC, Et_3N, CH_3CN; (iv) TFA/CH_2Cl_2 (70%).

Scheme 3. Synthesis of Phenylalanine and Tyrosine Hydroxamate Derivatives (**17a**−**r** and **18u**,**v**)[a]

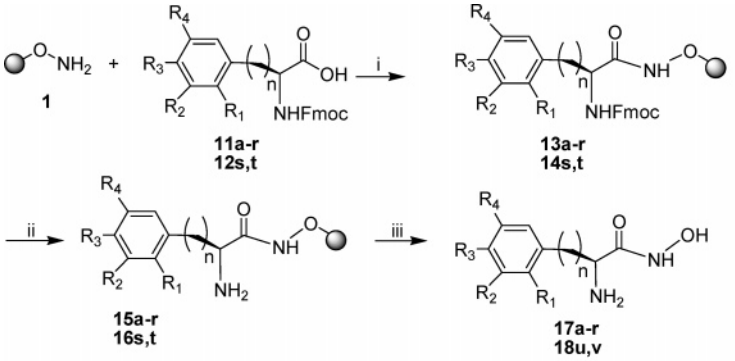

	R_1	R_2	R_3	R_4	n
a	H	H	NH_2	H	1
b	H	H	CN	H	1
c	H	H	N_3	H	1
d	H	H	$B(OH)_2$	H	1
e	H	H	NO_2	H	1
f	H	H	H	H	1
g	H	H	H	CH_3	1
h	H	H	$CH(CH_3)_2$	H	1
i	H	H	Ph	H	1
j	H	H	4-NO_2Ph	H	1
k	H	H	3-NO_2Ph	H	1
l	H	H	F	H	1
m	H	H	F	F	1
n	H	H	Cl	H	1
o	H	H	Br	H	1
p	H	H	I	H	1
q	I	H	H	H	1
r	H	I	OH	I	1
s	H	H	OtBu	H	0
t	H	H	OtBu	H	2
u	H	H	OH	H	0
v	H	H	OH	H	2

[a] Reagents: (i) HBTU, NMM/DMF (0.4 M); (ii) piperidine/DMF (20%); (iii) TFA/CH_2Cl_2 (70%).

Scheme 4. Synthesis of Tyrosine Hydroxamate Analogues with Modified α-Amino Group (−NH_2) (**23a**−**d**)[a]

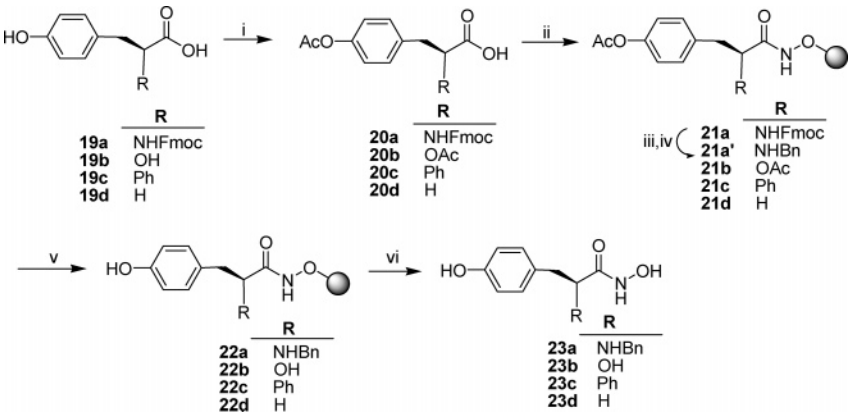

[a] Reagents: (i) Ac_2O, pyridine; (ii) **1**, HBTU, NMM/DMF (0.4 M); (iii) piperidine/DMF (20%); (iv) BnBr, pyridine; (v) NaOMe, MeOH; (vi) TFA/CH_2Cl_2 (70%).

inhibition, the role of the hydroxamate group was first examined. To further verify the importance of the hydroxamate functional group and its role as the metal binding motif in M2 mediated inhibition, the −CO, −NH, and −OH moieties of the hydroxamate group (−CO−NH−OH) were modified (Table 2).

When the hydroxamate group in **5a** was replaced with thiohydroxamate group in **5b**, the inhibitory potency was enhanced by approximately 4-fold, possibly because of the stronger binding affinity of sulfur to metals. N-Alkylation or N-arylation of the −NH group significantly reduced the inhibitory potency toward Csk as shown in *N*-methyl- and *N*-benzyltyrosine hydroxamate analogues (**5c** and **5d**).

L-Tyrosine (**5e**), which contains an −OH group instead of a −NHOH, did not inhibit Csk in the presence or the absence of Co^{2+} even at the high concentration of 1 mM. Additionally, replacement of the −OH group in the hydroxamate group by $-NH_2$ in L-tyrosine hydrazide (**5f**) reduced the inhibitory potency by approximately 8-fold.

Structure−activity relationships by these analogues revealed that moieties (−OH, −CO, or −NH) of the hydroxamate group are required for binding to Co^{2+}. These results further confirm that the −NHOH group plays key roles in the inhibition process involving the chelation with metal and/or interaction with the target binding site.

Table 1. Inhibition of Csk by Hydroxamates

	inhibition of Csk, %	
25 μM compd	12 mM $MgCl_2$	12 mM $MgCl_2$ + 0.2 mM $CoCl_2$
none	0	0
L-HisH	0	2
L-ArgH	0	36
L-LysH	3	26
L-TyrH	0	83
L-LeuH	4	62
β-AlaH	0	7
DL-NorvalH	0	40
DL-Asp γ-H	0	0
L-Glu γ-monoH	0	0
DL-PheH	0	77
GlyH	0	45

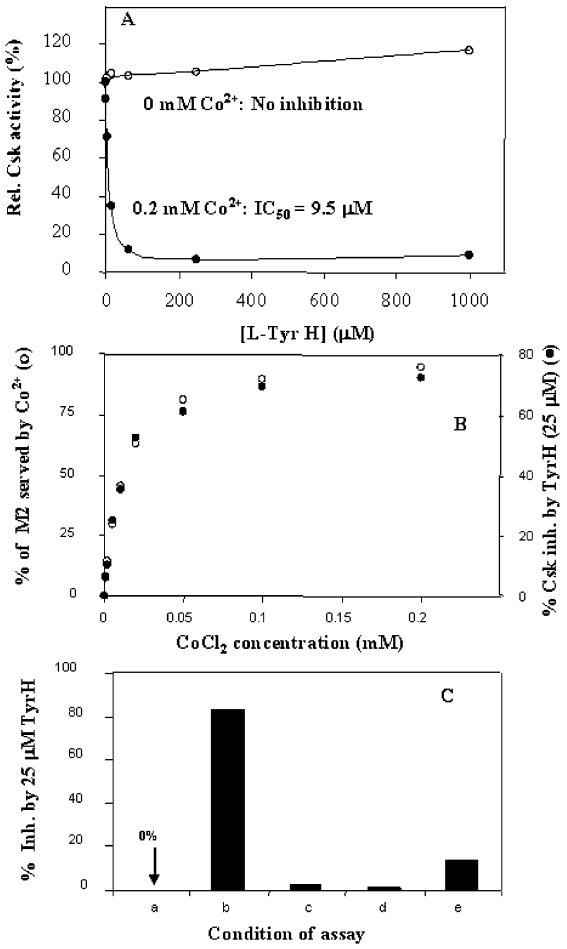

Figure 1. Characterization of Co^{2+}-dependent inhibition of Csk by L-TyrH. The data are the average of triplicate experiments. The upper limit of the standard error of the mean (SEM) was ±10%: (A) inhibition pattern of Csk in the presence of variable concentrations of L-TyrH and the presence or absence of Co^{2+}; (B) Co^{2+} concentration-dependent inhibition of Csk (l-TyrH = 25 μM, $MgCl_2$ = 12 mM); (C) Csk inhibition in the presence of different metals combinations, (a) 12 mM $MgCl_2$, (b) 12 mM Mg^{2+} and 0.2 mM Co^{2+}, (c) 12 mM $MgCl_2$ + 2 mM $MnCl_2$, (d) 2 mM $MnCl_2$, (e) 2 mM Mn^{2+} and 0.2 mM Co^{2+}.

II. Phenyl-Substituted Hydroxamate Analogues. The inhibition of Csk by TyrH, PheH, and LeuH suggests that a hydrophobic pocket on Csk near the M2 binding site is involved in the binding to these inhibitors. To optimize this interaction, different functional groups were introduced to the aryl ring of PheH to probe the interactions of the aryl ring with such a hydrophobic pocket. These substitution groups had different size, polarity, and charge and allowed us to systematically probe the binding environment of the aryl ring (Table 3).

Table 2. Inhibitory Potency of Class I Analogues Containing Modified Hydroxamate Functional Groups in the Presence of Co^{2+} (0.2 mM)

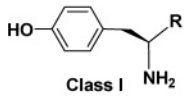

Class I

Compd	R	IC_{50} (μM)[a]
5a		9.5
5b		2.5
5c		no inhibition[b]
5d		291
5e		no inhibition[b]
5f	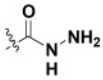	75

[a] IC_{50} is the concentration required to produce 50% inhibition in phosphorylation of poly-E_4Y by Csk (average of triplicate experiments). The upper limit of the standard error of the mean (SEM) was ±10%. [b] No inhibition up to 1000 μM.

Table 3. Inhibitory Potency of Phenyl-Substituted Analogues (Class II) in the Presence of Co^{2+} (0.2 mM)

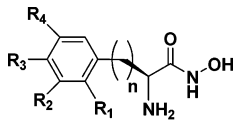

Classes II and III

compd	R_1	R_2	R_3	R_4	*n*	IC_{50} (μM)[a]
17a	H	H	NH_2	H	1	47
17b	H	H	CN	H	1	28
17c	H	H	N_3	H	1	21
17d	H	H	$B(OH)_2$	H	1	34
17e	H	H	NO_2	H	1	7
17f	H	H	H	H	1	15.5
17g	H	H	CH_3	H	1	9.5
17h	H	H	$CH(CH_3)_2$	H	1	3.3
17i	H	H	Ph	H	1	12
17j	H	H	4-NO_2Ph	H	1	4.9
17k	H	H	3-NO_2Ph	H	1	6.1
17l	H	H	F	H	1	11
17m	H	H	F	F	1	18
17n	H	H	Cl	H	1	6.3
17o	H	H	Br	H	1	5.6
17p	H	H	I	H	1	3.2
17q	I	H	H	H	1	3.4
17r	H	I	OH	I	1	3.4
18u	H	H	OH	H	0	57.0
18v	H	H	OH	H	2	18.0

[a] Average of triplicate experiments. The upper limit of the standard error of the mean (SEM) was ±10%.

Introducing polar groups (−NH_2, −CN, −N_3, −$B(OH)_2$) at the para position of the phenyl ring in **17a**−**d** in phenylalanine hydroxamates reduced the inhibitory potency (IC_{50} = 21−47 μM). On the other hand, introducing alkyl groups (CH_3, $CH(CH_3)_2$) at the para position of the phenyl ring in **17g** and **17h** gradually enhanced the inhibitory potency compared to **17f** according to the volume of the alkyl group.

Similar to the alkyl-substituted compounds, introducing bulkier halogens on the phenyl ring in **17n**−**p** enhanced the

Table 4. Inhibitory Potency of Tyrosine Hydroxamate Analogues Containing a Modified α-Amino Group (Class IV) in the Presence of Co^{2+} (0.2 mM)

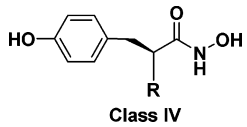

Class IV

compd	R	IC_{50} (μM)[a]
23a	NHBn	29
23b	OH	no inhibition[b]
23c	Ph	290
23d	H	no inhibition[b]

[a] Average of triplicate experiments. The upper limit of the standard error of the mean (SEM) was ±10%. [b] No inhibition up to 1000 μM.

inhibitory potency. For example, 4-iodo-substituted analogue (**17p**) showed approximately 3-fold higher inhibition compared to TyrH. These results indicate that by introduction of a bulkier group on the phenyl ring, the interaction between the hydroxamate analogues and a hydrophobic pocket of Csk enhances the inhibitory potency.

Compound **17i** (IC_{50} = 12 μM), which has an unsubstituted phenyl group perpendicular to the phenyl of phenylalanine hydroxamate, did not exhibit improved inhibitory potency compared to **17h**. Substitution of the phenyl group with NO_2 at the para and meta positions in compounds **17j** (IC_{50} = 4.9 μM) and **17k** (IC_{50} = 6.1 μM), respectively, showed enhanced inhibitory potency, possibly by changing the conformation of the substituted phenyl group to a more favorable position for interaction with the hydrophobic pocket.

III. Analogues with Modified Linker between Hydroxamate and Phenyl Functional Groups. Two TyrH derivatives were synthesized that had different $-(CH_2)_n-$ linker size between the hydroxamate group and the phenyl, where *n* is changed from 1 in TyrH **(5a)** to 0 and 2 in **18u** and **18v**, respectively (Table 3). Shortening or lengthening the distance between the hydroxamate group and the phenyl in **18u** and **18v** significantly reduced the inhibitory potency. These results suggest that an optimal distance is required between the hydrophobic side chain and hydroxamate group for a favorable interaction with the M2-binding site.

IV. TyrH Analogues with Modified α-Amino Group ($-NH_2$). To explore the role of α-amino group of TyrH in inhibition of Csk, compounds **23a**−**d** with modified α-amino group were synthesized (Table 4). The substitution on the α-amino group of TyrH with the benzyl group in **23a** led to 3-fold reduced inhibitory potency compared to **5a**. The replacement of α-amino group with −OH and −H in **23b** and **23d**, respectively, completely eliminated the inhibitory potency. Additionally, the replacement of an α-amino group with a phenyl group in **23c** reduced the inhibitory potency by 31-fold compared to **5a**. These results suggest that the presence of the α-amino group of TyrH is critical in generating inhibitory potency possibly through a favorable interaction with residues located in the kinase domain.

Hydroxamates and thiohydroxamates have been previously reported to create complexes with Co^{2+} and other transition metals.[24−30] On the basis of the structure−activity relationship data, it appears that the −CO, −NH, and −OH moieties in the hydroxamate group (−CONHOH) and the α-amino group are binding to Co^{2+} or M2 site. Structure−activity relationships by analogues in Table 2 revealed that replacement or elimination of −OH, −CO, or −NH moieties of the hydroxamate group significantly modified the inhibitory potencies against Csk. Furthermore, the replacement of α-amino group in TyrH with −OH and −H completely eliminated the inhibitory potency (Table 4), indicating the importance of this group. The exact nature of complexation between these groups and Co^{2+} or interaction with M2 remains unknown. It appears that a number of other factors in addition to complexation contribute to inhibitory potency. For example, by introduction of a bulkier group on the phenyl ring, the inhibitory potency was enhanced significantly (Table 3). Structure−activity relationships provide insights about the contribution of different functional groups in hydroxamate derivatives in metal-mediated inhibition. This led to a much better understanding of the inhibitory mechanism and improved inhibition. Structural studies of the enzyme−inhibitor complex is needed to determine the exact nature of the interactions of these functional groups with Csk and Co^{2+}.

Conclusions

This study established hydroxamate, represented by TyrH, as a scaffold for metal-mediated inhibitors against a protein tyrosine kinase and revealed a number of important structural features for the inhibition. To the best of our knowledge, this is the first reported design of metal-mediated inhibitors against protein tyrosine kinases by targeting a metal-binding site. Tyrosine thiohydroxamate (**5b**) and compounds containing hydrophobic residues on the phenyl ring (**17h** and **17p**−**r**) showed improved inhibitory potency compared to TyrH. Taken together, these results suggest that exploring further structural diversity of functional groups of hydroxamate analogues may lead to more potent Csk inhibitors. Additionally, this design strategy lays the foundation for developing metal-mediated inhibitors against other PTKs.

Experimental Section

Chemistry. All solid-phase reactions were carried out in Bio-Rad polypropylene columns by shaking and mixing at room temperature using a Glass-Col small tube rotator under dry conditions unless otherwise stated. Real-time monitoring of loading of compounds on resin beads was carried out with a Thermo-Nicolet 550 FT-IR spectrophotometer coupled with a Nic-Plan microscope using OMNIC software. The chemical structures of final products were characterized by nuclear magnetic resonance spectra (^1H NMR, ^{13}C NMR) determined on a Bruker NMR spectrometer (400 MHz). ^{13}C NMR spectra are fully decoupled. Chemical shifts were reported in parts per millions (ppm). The chemical structures of final products were confirmed by a high-resolution PE Biosystems Mariner API time-of-flight electrospray mass spectrometer. Final compounds were purified (>99%) on a Phenomenex Prodigy 10 μm ODS reversed-phase column (2.1 cm × 25 cm) with a Hitachi HPLC system using a gradient system of acetonitrile and water (CH_3CN/H_2O, 0−40%, pH 7.0, 30 min). The purity of final products (>99%) was confirmed by analytical HPLC. The analytical HPLC was performed on the Hitachi analytical HPLC system on a C18 Shimadzu Premier 3 μm column (150 cm × 4.6 mm) using two different isocratic systems and a flow rate of 1 mL/min with UV detection at 260 nm. L-Tyrosine (**5e**), L.-HisH, L-ArgH, l-LysH, L-LeuH, β-AlaH, DL-NorvalH, DL-Asp γ-H, L-Glu γ-monoH, DL-PheH, and GlyH were purchased from Sigma-Aldrich Co. L-Tyrosine hydrazide (**5f**) was purchased from MP Biomedicals Co.

General Procedure for the Synthesis of 5a,b, 17a-r, and 18u,v. Hydroxylamine Wang resin (**1**, 50 mg, 2 mmol/g) was swollen in DMF (5 mL) for 15 min. *N*-(9-Fluorenylmethoxycarbonyl)-L-phenylalanine analogues (**2**, **11a**−**r**, or **12s**,**t**; 0.4 mmol) and HBTU (170 mg, 0.5 mmol) were dissolved in NMM/DMF (5 mL, 0.4 M) and added to the swollen resin. The reaction mixture was shaken for 30 min. The resin was collected by filtration and washed successively with DMF (3 × 5 mL), dichloromethane (3 × 5 mL), and methanol (2 × 5 mL) to afford **3a**, **13a**−**r**, and **14s**,**t**,

respectively. The resin **3a** (50 mg, 0.1 mmol) was swollen in THF (15 mL) for 10 min. Lawesson's reagent (121 mg, 0.3 mmol) was added to the swollen resin. The reaction mixture was shaken for 3 days. The resin was collected by filtration and washed successively with DMF (3 × 5 mL) and methanol (2 × 5 mL) to afford **3b**. Piperidine in DMF (5 mL, 20%) was added to **3a**, **3b**, **13a**−**r**, and **14s**,**t**, and the reaction mixture was shaken for 10 min. The resins were collected by filtration, washed successively with DMF (3 × 5 mL), dichloromethane (3 × 5 mL), and methanol (2 × 5 mL) to give **4a**,**b**, **15a**−**r**, and **16s**,**t**. The cleavage was carried out by addition of TFA in dichloromethane (70%, 5 mL). After 30 min of shaking of the mixtures at room temperature, the resins were collected by filtration. The solvents of filtrate solutions were evaporated, and the residues were dried under vacuum. The crude mixtures were purified by HPLC as described above to yield **5a**,**b**, **17a**−**r**, and **18u**,**v**, respectively (overall yield, 30−60%).

General Procedure for the Synthesis of 5c,d. Wang resin (**6**, 100 mg; 1.1 mmol/g) was swollen in dichloromethane (5 mL) for 15 min. *N*-(9-Fluorenylmethoxycarbonyl)-L-tyrosine methyl ester (210 mg, 0.5 mmol) and triphenylphosphine (144 mg, 0.54 mmol) were dissolved in dichloromethane (2 mL) and added to the swollen resin. Diispropylazodicarboxylate (DIAD, 90 μL, 0.47 mmol) was diluted to 400 μL with dichloromethane and added dropwise to the mixture at room temperature. The reaction mixture was shaken overnight. The resin was collected by filtration, washed successively with dichloromethane (5 mL), DMF (3 × 5 mL), and methanol (2 × 5 mL), and dried under vacuum to afford **8**. The solution of sodium hydroxide in methanol (6 mL, 0.4 M) was added to the dried resin, and the reaction mixture was shaken for 6 days. The resin was collected by filtration, washed successively with DMF (3 × 5 mL), dichloromethane (3 × 5 mL), and methanol (2 × 5 mL), and dried under vacuum to give **9**. The resin was swollen in THF (5 mL) for 15 min. *N*-Methylhydroxylamine hydrochloride or *N*-benzylhydroxylamine hydrochloride (RNHOH·HCl, 0.6 mmol) and diisopropylcarbodiimide (93 μL, 0.6 mmol) were added to the swollen resin and mixed. Triethylamine (Et_3N, 18 μL, 1.3 mmol) was added to the mixture. The reaction mixture was shaken overnight. The resin was collected by filtration and washed successively with DMF (3 × 5 mL), dichloromethane (3 × 5 mL), and methanol (2 × 5 mL) to afford **10a** or **10b**. The cleavage was carried out by addition of TFA in dichloromethane (70%, 5 mL) to **10a** or **10b**. After 30 min of shaking of the mixtures at room temperature, the resins were collected by filtration and washed with dichloromethane (2 mL). The solvents of filtrate solutions were evaporated, and the residues were dried under vacuum. The crude mixtures were purified by HPLC as described above to yield **5c** or **5d** (overall yield, ∼18−20%).

General Procedure for the Synthesis of 23a−**d.** To (*S*)-3-(4-hydroxylphenyl)propionic acid derivatives (**19a**−**d**) (0.5 mmol) in dry pyridine (4 mL) was added acetic anhydride (Ac_2O, 2 mL). The reaction mixtures were stirred at room temperature overnight. The solvent was removed under vacuum, and the mixtures were purified by silica gel column chromatography using hexane and ethyl acetate as eluents to yield (*S*)-3-(4-acetoxylphenyl)propionic acid derivatives (**20a**−**d**). HBTU (170 mg, 0.5 mmol) and **20a**−**d** were dissolved in the NMM/DMF (5 mL, 0.4 M) and added to the swollen hydroxylamine Wang resin (50 mg; loading, 2.0 mmol/g). The reaction mixtures were shaken for 30 min. The resins were collected by filtration and washed successively with DMF (3 × 5 mL), dichloromethane (3 × 5 mL), and methanol (2 × 5 mL) to give **21a**−**d**. The Fmoc group in **21a** was removed by piperidine in DMF (20%). To the resulting polymer-bound unprotected amine was added benzyl bromide (0.5 mL, 4 mmol) in dry pyridine (5 mL). The mixture was shaken overnight. The resin was collected by filtration and washed successively with DMF (3 × 5 mL), dichloromethane (3 × 5 mL), and methanol (2 × 5 mL) to afford **21a′**. The acetyl groups in **21a′**, **21b**, **21c**, and **21d** were removed by addition of sodium methoxide (20 mg) in methanol (5 mL). The mixtures were shaken for 2 h. The resins were collected by filtration and washed successively with DMF (3 × 5 mL), dichloromethane (3 × 5 mL), and methanol (2 × 5 mL) to give **22a**−**d**. The cleavage was carried out by addition of TFA in dichloromethane (70%, 5 mL). After 30 min of shaking of the mixtures at room temperature, the resins were collected by filtration and washed with dichloromethane (2 mL). The solvents of filtrate solutions were evaporated, and the residues were dried under vacuum. The crude mixtures were purified by HPLC as described above to yield **23a**−**d** (overall yield, 25−30%).

(*S*)-2-Amino-*N*-hydroxy-3-(4-hydroxyphenyl)propanethioamide (5b). ^{1}H NMR (DMSO-d_6, 400 MHz, δ ppm): 2.75−2.85 (m, 1H, CH_2), 3.12−3.25 (m, 1H, CH_2), 3.60−3.75 (m, 1H, C*H*), 6.63 (d, *J* = 8.00 Hz, 2H, aromatic H), 6.99 (d, *J* = 8.00 Hz, 2H, aromatic H), 7.85 (br s, 2H, NH_2), 9.10 (s, 1H, O*H*), 9.22 (s, 1H, O*H*). ^{13}C NMR (DMSO-d_6, 100 MHz, δ ppm): 38.07, 59.31, 115.80, 127.44, 131.17, 156.84, 166.40. HR-MS (ESI-TOF) (*m*/*z*): $C_9H_{12}N_2O_2S$ calcd, 212.0619; found, 213.2830 $[M + 1]^+$, 214.2910 $[M + 2]^+$.

(*S*)-2-Amino-*N*-hydroxy-3-(4-hydroxyphenyl)-*N*-methylpropanamide (5c). ^{1}H NMR (DMSO-d_6, 400 MHz, δ ppm): 2.88−2.94 (m, 1H, CH_2), 3.09−3.13 (m, 1H, CH_2), 3.15 (s, 3H, CH_3), 4.34−4.38 (m, 1H, C*H*), 6.71 (d, *J* = 8.40 Hz, 2H, aromatic H), 7.01 (d, *J* = 8.40 Hz, 2H, aromatic H), 8.13 (s, 2H, NH_2), 9.42 (s, 1H, O*H*), 10.84 (s, 1H, O*H*). ^{13}C NMR (DMSO-d_6, 100 MHz, δ ppm): 35.23, 36.87, 52.41, 116.23, 125.76, 131.39, 157.43, 168.28. HR-MS (ESI-TOF) (*m*/*z*): $C_{10}H_{14}N_2O_3$ calcd, 210.1004; found, 211.3252 $[M + 1]^+$, 212.355 $[M + 2]^+$.

(*S*)-2-Amino-*N*-benzyl-*N*-hydroxy-3-(4-hydroxyphenyl)propanamide (5d). ^{1}H NMR (DMSO-d_6, 400 MHz, δ ppm): 2.83−2.87 (m, 1H, CH_2), 3.04−3.08 (m, 1H, CH_2), 4.36−4.40 (m, 1H, C*H*), 4.75 (s, 2H, CH_2), 6.69 (d, *J* = 7.60 Hz, 2H, aromatic H), 6.97 (d, *J* = 7.60 Hz, 2H, aromatic H), 7.30−7.36 (m, 5H, aromatic H), 7.97 (br s, 2H, NH_2), 9.38 (s, 1H, O*H*), 10.57 (s, 1H, O*H*). ^{13}C NMR (DMSO-d_6, 100 MHz, δ ppm): 35.48, 52.59, 116.26, 125.63, 128.40, 129.03, 129.26, 131.43, 138.80, 157.47, 168.85. HR-MS (ESI-TOF) (*m*/*z*): $C_{16}H_{18}N_2O_3$ calcd, 286.1317; found, 287.2736 $[M + 1]^+$, 288.3632 $[M + 2]^+$.

(*S*)-2-Amino-3-(4-aminophenyl)-*N*-hydroxypropanamide (17a). ^{1}H NMR (DMSO-d_6, 400 MHz, δ ppm): 2.83−2.87 (m, 2H, CH_2), 3.62 (t, *J* = 7.00 Hz, 1H, C*H*), 5.63 (br s, 2H, NH_2), 6.55 (d, *J* = 8.00 Hz, 2H, aromatic H), 6.87 (d, *J* = 8.00 Hz, 2H, aromatic H), 8.23 (s, 2H, NH_2), 9.26 (s, 1H, OH), 10.94 (s, 1H, NH). ^{13}C NMR (DMSO-d_6, 100 MHz, δ ppm): 37.22, 52.89, 115.61, 123.27, 130.75, 147.25, 165.23. HR-MS (ESI-TOF) (*m*/*z*): $C_9H_{13}N_3O_2$ calcd, 195.1008; found, 196.3336 $[M + 1]^+$, 244.3152 $[M + 2]^+$.

(*S*)-2-Amino-3-(4-cyanophenyl)-*N*-hydroxypropanamide (17b). ^{1}H NMR (DMSO-d_6, 400 MHz, δ ppm): 3.05−3.10 (m, 2H, CH_2), 3.81−3.84 (m, 1H, C*H*), 7.41 (d, *J* = 8.00 Hz, 2H, aromatic H), 7.82 (d, *J* = 8.00 Hz, 2H, aromatic H), 8.40 (br s, 2H, NH_2), 9.31 (br s, 1H, O*H*), 11.01 (s, 1H, N*H*). HR-MS (ESI-TOF) (*m*/*z*): $C_{10}H_{11}N_3O_2$ calcd, 205.0851; found, 206.2166 $[M + 1]^+$.

(*S*)-2-Amino-3-(4-azidophenyl)-*N*-hydroxypropanamide (17c). ^{1}H NMR (DMSO-d_6, 400 MHz, δ ppm): 2.94−2.99 (m, 2H, CH_2), 3.69−3.74 (m, 1H, C*H*), 7.10 (d, *J* = 8.40 Hz, 2H, aromatic H), 7.24 (d, *J* = 8.40 Hz, 2H, aromatic H), 8.28 (br s, 2H, NH_2), 9.29 (s, 1H, O*H*), 10.95 (s, 1H, N*H*). HR-MS (ESI-TOF) (*m*/*z*): $C_9H_{11}N_5O_2$ calcd, 221.0913; found, 222.2411 $[M + 1]^+$, 223.2430 $[M + 2]^+$.

4-((*S*)-2-(Hydroxycarbamoyl)-2-aminoethyl)phenylboronic Acid (17d). ^{1}H NMR (DMSO-d_6, 400 MHz, δ ppm): 2.80−3.20 (m, 2H, CH_2), 3.68−3.72 (m, 1H, C*H*), 7.12−7.22 (m, 2H, aromatic H), 7.72−7.78 (m, 2H, aromatic H), 8.0 (s, 2H, BO*H*), 8.28 (br s, 2H, NH_2), 9.28 (s, 1H, O*H*), 10.95 (s, 1H, N*H*). HR-MS (ESI-TOF) (*m*/*z*): $C_9H_{13}BN_2O_4$ calcd, 224.0968; found, 224.2403 $[M]^+$, 225.2274 $[M + 1]^+$.

(*S*)-2-Amino-*N*-hydroxy-3-(4-nitrophenyl)propanamide (17e). ^{1}H NMR (DMSO-d_6, 400 MHz, δ ppm): 3.00−3.10 (m, 2H, CH_2), 3.73−3.77 (m, 1H, C*H*), 7.50 (d, *J* = 8.80 Hz, 2H, aromatic H), 7.81 (br s, 2H, NH_2), 8.22 (d, *J* = 8.80 Hz, 2H, aromatic H), 9.25 (br s, 1H, O*H*), 10.90 (br s, 1H, N*H*). ^{13}C NMR (DMSO-d_6, 100 MHz, δ ppm): 37.80, 52.32, 124.46, 131.74, 144.14, 147.63, 165.12. HR-MS (ESI-TOF) (*m*/*z*): $C_9H_{11}N_3O_4$ calcd, 225.0749; found, 226.2678 $[M + 1]^+$, 227.2962 $[M + 2]^+$.

(*S*)-2-Amino-*N*-hydroxy-3-phenylpropanamide (17f). ^{1}H NMR (DMSO-d_6, 400 MHz, δ ppm): 2.87−3.10 (m, 2H, CH_2), 3.75 (t, J = 7.00 Hz, 1H, CH), 7.20−7.25 (m, 2H, aromatic H), 7.26−7.37 (m, 3H, aromatic H), 8.30 (br s, 2H, NH_2), 9.30 (s, 1H, OH), 10.98 (s, 1H, NH). ^{13}C NMR (DMSO-d_6, 100 MHz, δ ppm): 37.84, 52.57, 128.05, 129.45, 130.23, 135.73, 165.00. HR-MS (ESI-TOF) (m/z): $C_9H_{12}N_2O_2$ calcd, 180.0899; found, 181.3126 [M + 1]$^+$, 182.3207 [M + 2]$^+$.

(*S*)-2-Amino-*N*-hydroxy-3-*p*-tolylpropionamide (17g). ^{1}H NMR (DMSO-d_6, 400 MHz, δ ppm): 2.29 (s, 3H, CH_3), 2.86−2.99 (m, 2H, CH_2), 3.72 (t, J = 7.00 Hz, 1H, CH), 7.05−7.17 (m, 4H, aromatic H), 8.26 (br s, 2H, NH_2), 9.29 (s, 1H, OH), 10.96 (s, 1H, NH). ^{13}C NMR (DMSO-d_6, 100 MHz, δ ppm): 21.53, 37.44, 52.64, 130.00, 130.10, 132.64, 137.09, 165.05. HR-MS (ESI-TOF) (m/z): $C_{10}H_{14}N_2O_2$ calcd, 194.1055; found, 195.3455 [M + 1]$^+$, 196.3175 [M + 2]$^+$.

(*S*)-2-Amino-*N*-hydroxy-3-(4-isopropylphenyl)propanamide (17h). ^{1}H NMR (DMSO-d_6, 400 MHz, δ ppm): 1.19 (d, 6H, CH_3), 2.83−2.90 (m, 2H, CH_2), 2.90−3.03 (m, 1H, CH), 3.69−3.74 (m, 1H, CH), 7.13 (d, 2H, J = 8.00 Hz, aromatic H), 7.21 (d, J = 8.00 Hz, 2H, aromatic H), 8.17 (br s, 2H, NH_2), 9.29 (s, 1H, OH), 10.96 (s, 1H, NH). HR-MS (ESI-TOF) (m/z): $C_{12}H_{18}N_2O_2$ calcd, 222.1368; found, 223.1797 [M + 1]$^+$, 224.1997 [M + 2]$^+$.

(*S*)-2-Amino-*N*-hydroxy-3-[4-(phenyl)phenyl]propanamide (17i). ^{1}H NMR (DMSO-d_6, 400 MHz, δ ppm): 3.01−3.08 (m, 2H, CH_2), 3.73−3.81 (m, 1H, CH), 7.25−7.40 (m, 2H, aromatic H), 7.42−7.50 (m, 2H, aromatic H), 7.60−7.70 (m, 5H, aromatic H), 8.24 (br s, 2H, NH_2), 9.31 (s, 1H, OH), 10.98 (s, 1H, NH). HR-MS (ESI-TOF) (m/z): $C_{15}H_{17}N_2O_2$ calcd, 256.1212; found, 257.2748 [M + 1]$^+$.

(*S*)-2-Amino-*N*-hydroxy-3-[4-(nitrophenyl)phenyl]propanamide (17j). ^{1}H NMR (DMSO-d_6, 400 MHz, δ ppm): 3.01−3.12 (m, 2H, CH_2), 3.79−3.83 (m, 1H, CH), 7.34−7.43 (m, 2H, aromatic H), 7.76−7.83 (m, 2H, aromatic H), 7.91−8.00 (m, 2H, aromatic H), 8.27−8.38 (m, 4H, aromatic H and NH_2), 9.33 (s, 1H, OH), 11.01 (s, 1H, NH). HR-MS (ESI-TOF) (m/z): $C_{15}H_{15}N_3O_4$ calcd, 301.1063; found, 302.4769 [M + 1]$^+$.

(*S*)-2-Amino-*N*-hydroxy-3-[3-(nitrophenyl)phenyl]propanamide (17k). ^{1}H NMR (DMSO-d_6, 400 MHz, δ ppm): 3.00−3.13 (m, 2H, CH_2), 3.76−3.86 (m, 1H, CH), 7.35−7.42 (m, 2H, aromatic H), 7.72−7.82 (m, 3H, aromatic H), 8.11−8.20 (m, 1H, aromatic H), 8.22−8.26 (m, 1H, aromatic H), 8.34 (br s, 2H, NH_2), 8.40−8.45 (m, 1H, aromatic H), 9.34 (s, 1H, OH), 11.02 (s, 1H, NH). HR-MS (ESI-TOF) (m/z): $C_{15}H_{15}N_3O_4$ calcd, 301.1063; found, 302.4702 [M + 1]$^+$.

(*S*)-2-Amino-3-(4-fluorophenyl)-*N*-hydroxypropanamide (17l). ^{1}H NMR (DMSO-d_6, 400 MHz, δ ppm): 2.90−3.05 (m, 2H, CH_2), 3.75 (t, J = 7.20 Hz, 1H, CH), 7.10−7.30 (m, 4H, aromatic H), 8.30 (br s, 2H, NH_2), 9.31 (s, 1H, OH), 10.99 (s, 1H, NH). ^{13}C NMR (DMSO-d_6, 100 MHz, δ ppm): 36.97, 52.58, 116.30, 132.16, 132.24, 163.55, 164.96. HR-MS (ESI-TOF) (m/z): $C_9H_{11}FN_2O_2$ calcd, 198.0805; found, 199.2988 [M + 1]$^+$.

(*S*)-2-Amino-3-(3,4-difluorophenyl)-*N*-hydroxypropanamide (17m). ^{1}H NMR (DMSO-d_6, 400 MHz, δ ppm): 2.85−3.10 (m, 2H, CH_2), 3.74 (t, J = 7.0 Hz, 1H, CH), 7.00−7.10 (m, 1H, aromatic H), 7.20−7.30 (m, 1H, aromatic H), 7.42−7.46 (m, 1H, aromatic H), 7.92 (br s, 2H, NH_2), 9.26 (s, 1H, OH), 10.88 (br s, 1H, NH). ^{13}C NMR (DMSO-d_6, 100 MHz, δ ppm): 37.24, 52.58, 118.28, 118.45, 119.17, 119.34, 127.20, 127.27, 165.44. HR-MS (ESI-TOF) (m/z): $C_9H_{10}F_2N_2O_2$ calcd, 216.0710; found, 217.2563 [M + 1]$^+$.

(*S*)-2-Amino-3-(4-chlorophenyl)-*N*-hydroxypropanamide (17n). ^{1}H NMR (DMSO-d_6, 400 MHz, δ ppm): 2.90−3.05 (m, 2H, CH_2), 3.75 (t, J = 7.00 Hz, 1H, CH), 7.23 (d, J = 8.40 Hz, 2H, aromatic H), 7.40 (d, 2H, J = 8.40 Hz, aromatic H), 8.30 (br s, 2H, NH_2), 9.31 (s, 1H, OH), 10.99 (s, 1H, NH). ^{13}C NMR (DMSO-d_6, 100 MHz, δ ppm): 37.11, 52.43, 129.38, 132.16, 132.80, 134.76, 164.88. HR-MS (ESI-TOF) (m/z): $C_9H_{11}ClN_2O_2$ calcd, 214.0509; found, 215.2769 [M + 1]$^+$, 217.2745 [M + 2]$^+$.

(*S*)-2-Amino-3-(4-bromophenyl)-*N*-hydroxypropionamide (17o). ^{1}H NMR (DMSO-d_6, 400 MHz, δ ppm): 2.88−3.01 (m, 2H, CH_2), 3.72 (t, J = 7.20 Hz, 1H, CH), 7.16 (d, J = 8.00 Hz, 2H, aromatic H), 7.54 (d, J = 8.00 Hz, 2H, aromatic H), 8.11 (br s, 2H, NH_2), 9.22 (s, 1H, OH), 10.94 (s, 1H, NH). ^{13}C NMR (DMSO-d_6, 100 MHz, δ ppm): 37.31, 52.41, 121.35, 132.43, 132.50, 135.25, 165.08. HR-MS (ESI-TOF) (m/z): $C_9H_{11}BrN_2O_2$ calcd, 258.0004; found, 259.1935 [M + 1]$^+$, 261.1879 [M + 2]$^+$.

(*S*)-2-Amino-*N*-hydroxy-3-(4-iodophenyl)propanamide (17p). ^{1}H NMR (DMSO-d_6, 400 MHz, δ ppm): 2.90−3.10 (m, 2H, CH_2), 3.70−3.77 (m, 1H, CH), 7.02 (d, J = 8.00 Hz, 2H, aromatic H), 7.69 (d, J = 8.00 Hz, 2H, aromatic H), 8.28 (br s, 2H, NH_2), 9.31 (s, 1H, OH), 10.99 (s, 1H, NH). ^{13}C NMR (DMSO-d_6, 100 MHz, δ ppm): 37.33, 52.37, 94.29, 132.65, 135.51, 138.15, 164.90. HR-MS (ESI-TOF) (m/z): $C_9H_{11}IN_2O_2$ calcd, 305.9865; found, 307.1113 [M + 2]$^+$.

(*S*)-2-Amino-*N*-hydroxy-3-(2-iodophenyl)propanamide (17q). ^{1}H NMR (DMSO-d_6, 400 MHz, δ ppm): 3.08−3.20 (m, 2H, CH_2), 3.70−3.80 (m, 1H, CH), 7.01−7.09 (m, 1H, aromatic H), 7.20−7.25 (m, 1H, aromatic H), 7.35−7.40 (m, 1H, aromatic H), 7.85−7.92 (m, 1H, aromatic H), 8.48 (br s, 2H, NH_2), 9.27 (s, 1H, OH), 10.94 (s, 1H, NH). HR-MS (ESI-TOF) (m/z): $C_9H_{11}IN_2O_2$ calcd, 305.9865; found, 307.1118 [M + 2]$^+$.

(*S*)-2-Amino-*N*-hydroxy-3-(4-hydroxy-3,5-diiodophenyl)propanamide (17r). ^{1}H NMR (DMSO-d_6, 400 MHz, δ ppm): 2.72−2.92 (m, 2H, CH_2), 3.68−3.75 (m, 1H, CH), 7.58 (br s, 2H, aromatic H), 8.22 (br s, 2H, NH_2), 9.34 (s, 1H, OH), 10.95 (s, 1H, NH). ^{13}C NMR (DMSO-d_6, 100 MHz, δ ppm): 35.78, 52.55, 88.09, 131.76, 140.69, 155.45, 165.03. HR-MS (ESI-TOF) (m/z): $C_9H_{10}I_2N_2O_3$ calcd, 447.8781; found, 448.7776 [M + 1]$^+$.

(*S*)-2-Amino-*N*-hydroxy-2-(4-hydroxyphenyl)acetamide (18u). ^{1}H NMR (DMSO-d_6, 400 MHz, δ ppm): 4.57−4.64 (m, 1H, CH), 6.75−6.85 (m, 2H, aromatic H), 7.25−7.35 (d, 2H, aromatic H), 8.52 (s, 2H, NH_2), 9.26 (s, 1H, OH), 9.77 (s, 1H, OH), 11.08 (s, 1H, NH). HR-MS (ESI-TOF) (m/z): $C_8H_{10}N_2O_3$ calcd, 182.0691; found, 183.6436 [M + 1]$^+$, 205.5888 [M + Na]$^+$, 221.5359 [M + K]$^+$.

(*S*)-2-Amino-*N*-hydroxy-4-(4-hydroxyphenyl)butanamide (18v). ^{1}H NMR (DMSO-d_6, 400 MHz, δ ppm): 1.89−2.09 (m, 2H, CH_2), 2.10−2.16 (m, 2H, CH_2), 3.45−3.60 (m, 1H, CH), 6.60 (d, J = 7.60 Hz, 2H, aromatic H), 6.90 (d, 2H, aromatic H), 8.30 (br s, 2H, NH_2), 9.29 (s, 1H, OH), 9.38 (s, 1H, OH), 11.10 (s, 1H, NH). HR-MS (ESI-TOF) (m/z): $C_{10}H_{14}N_2O_3$ calcd, 210.1004; found, 211.0421 [M + 1]$^+$.

(*S*)-2-Benzylamino-*N*-hydroxy-3-(4-hydroxyphenyl)propanamide (23a). ^{1}H NMR (DMSO-d_6, 400 MHz, δ ppm): 2.60−2.78 (m, 2H, CH_2), 3.00−3.11 (m, 1H, CH_2), 3.47−3.52 (m, 1H, CH_2), 3.67−3.74 (m, 1H, CH), 6.64 (d, J = 8.40 Hz, 2H, aromatic H), 6.97 (d, J = 8.40 Hz, 2H, aromatic H), 7.17−7.30 (m, 5H, aromatic H), 8.81 (s, 1H, NH), 9.14 (s, 1H, OH), 10.45 (s, 1H, NH). HR-MS (ESI-TOF) (m/z): $C_{16}H_{18}N_2O_3$ calcd, 286.1317; found, 287.1699 [M + 1]$^+$, 288.2465 [M + 2]$^+$.

(*S*)-*N*,2-Dihydroxy-3-(4-hydroxyphenyl)propanamide (23b). ^{1}H NMR (DMSO-d_6, 400 MHz, δ ppm): 2.50−2.63 (m, 1H, CH_2), 2.70−2.85 (m, 1H, CH_2), 3.80−3.95 (m, 1H, CH), 5.20−5.30 (d, J = 6.40 Hz, 1H, OH), 6.65 (d, J = 8.00 Hz, 2H, aromatic H), 6.99 (d, J = 8.00 Hz, 2H, aromatic H), 8.70 (s, 1H, OH), 9.10 (s, 1H, OH), 10.40 (s, 1H, NH). HR-MS (ESI-TOF) (m/z): $C_9H_{11}NO_4$: calcd, 197.0688; found, 198.2101 [M + 1]$^+$.

(*S*)-*N*-Hydroxy-3-(4-hydroxyphenyl)-2-phenylpropanamide (23c). ^{1}H NMR (DMSO-d_6, 400 MHz, δ ppm): 2.76 (dd, J = 6.00 Hz, J = 13.60 Hz, 1H, CH_2), 3.19 (dd, J = 9.20 Hz, J = 13.60 Hz, 1H, CH_2), 3.49 (dd, J = 6.00 Hz, J = 9.20 Hz, 1H, CH), 6.61 (d, J = 8.40 Hz, 2H, aromatic H), 6.95 (d, J = 8.40 Hz, 2H, aromatic H), 7.20−7.40 (m, 5H, aromatic H), 8.74 (br s, 1H, OH), 9.14 (s, 1H, OH), 10.55 (s, 1H, NH). ^{13}C NMR (DMSO-d_6, 100 MHz, δ ppm): 38.40, 51.30, 115.74, 127.53, 128.60, 128.98, 130.50, 130.57, 141.42, 156.40. HR-MS (ESI-TOF) (m/z): $C_{15}H_{15}NO_3$ calcd, 257.1052; found, 258.2814 [M + 1]$^+$, 259.2742 [M + 2]$^+$.

***N*-Hydroxy-3-(4-hydroxyphenyl)propanamide (23d).** ^{1}H NMR (DMSO-d_6, 400 MHz, δ ppm): 2.16 (t, J = 7.20 Hz, 2H, CH_2), 2.69 (t, J = 7.20 Hz, 2H, CH_2), 6.63 (d, J = 8.40 Hz, 2H, aromatic

H), 6.95 (d, $J = 8.40$ Hz, 2H, aromatic H), 8.68 (s, 1H, O*H*), 9.14 (s, 1H, O*H*), 10.33 (s, 1H, N*H*). ^{13}C NMR (DMSO-d_6, 100 MHz, δ ppm): 30.96, 35.23, 115.87, 129.92, 131.95, 156.33, 169.23. HR-MS (ESI-TOF) (*m*/*z*): $C_9H_{11}NO_3$ calcd, 181.0739; found, 182.2973 $[M + 1]^+$, 183.3021 $[M + 2]^+$, 204.2666 $[M + Na]^+$, 220.2325 $[M + K]^+$.

Kinase Activity Assays. PTK activities were determined by measuring the phosphorylation of poly-E_4Y by the kinase using an acid precipitation assay as previously described.[8,10] The standard reaction contained the appropriate amount of the kinase, 1 mg mL^{-1} poly-E_4Y and 0.2 mM [^{32}P]-ATP (1,000 dpm pmol^{-1}) in the kinase assay buffer (75 mM EPPS, pH 8.0, 12 mM $MgCl_2$, 5% glycerol, 0.005% Triton X-100). The appropriate amount of kinase was predetermined to ensure that the kinase activity was linear with the amount of enzyme added. The reaction volume was 50 μL, and the reaction was allowed to proceed for 30 min at 30 °C. At the end of the reaction, 35 μL of the reaction mixture was spotted into a strip of filter paper (1 cm × 2 cm), and the reaction was stopped by immersing the filter paper in warm 5% TCA. The filter paper was washed three times in 5% TCA for 10 min each. Phosphorylated and unphosphorylated poly-E_4Y were both precipitated into the filter paper, and the amount of phosphate incorporated onto poly-E_4Y was determined by liquid scintillation counting.

To determine the inhibition of Csk by a hydroxamate compound, the reaction mixture also contained 0.2 mM $CoCl_2$ and various concentrations of the compound. To determine the effect of other metal cations on the inhibition, other metal salts were used in the place of $CoCl_2$. When the K_m and K_{cat} were determined with regard to one substrate, the kinase activity was determined at various concentrations of that substrate in the range of 20−200 μM for ATP or 20−200 μg mL^{-1} for poly-E_4Y. The K_{cat} and K_m values were determined by Lineweaver−Burk plots with linear regression using the Microsoft Excel program.

Acknowledgment. We acknowledge the financial support from American Cancer Society (Grant RSG CDD-106966).

Supporting Information Available: ^{1}H NMR and ^{13}C NMR spectra for representative compounds in different classes and their analytical HPLC profiles in two diverse systems. This material is available free of charge via the Internet at http://pubs.acs.org.

References

(1) Hubbard, S. R.; Till, J. H. Protein tyrosine kinase structure and function. *Annu. Rev. Biochem.* **2000**, *69*, 373−398.
(2) Hunter, T. Protein kinases and phosphatases: the yin and yang of protein phosphorylation and signaling. *Cell* **1995**, *27*, 225−236.
(3) Biscardi, J. S.; Tice, D. A.; Parsons, S. J. c-Src, receptor tyrosine kinases, and human cancer. *Adv Cancer Res.* **1999**, *76*, 61−119.
(4) Uckun, F. M.; Mao, C. Tyrosine kinases as new molecular targets in treatment of inflammatory disorders and leukemia. *Curr. Pharm. Des.* **2004**, *10*, 1083−1091.
(5) Thiesing, J. T.; Ohno-Jones, S.; Kolibaba, K. S.; Druker, B. J. Efficacy of STI571, an abl tyrosine kinase inhibitor, in conjunction with other antileukemic agents against bcr-abl-positive cells. *Blood* **2000**, *96*, 3195−3199.
(6) Wakeling, A. E.; Guy, S. P.; Woodburn, J. R.; Ashton, S. E.; Curry, B. J.; Barker, A. J.; Gibson, K. H. ZD1839 (Iressa): an orally active inhibitor of epidermal growth factor signaling with potential for cancer therapy. *Cancer Res.* **2002**, *62*, 5749−5754.
(7) Stout, T. J.; Foster, P. G.; Matthews, D. J. High-throughput structural biology in drug discovery: protein kinases. *Curr. Pharm. Des.* **2004**, *10*, 1069−1082.
(8) Sun, G.; Budde, R. J. Requirement for an additional divalent metal cation to activate protein tyrosine kinases. *Biochemistry* **1997**, *36*, 2139−2146.
(9) Sun, G.; Budde, R. J. Expression, purification and initial characterization of human Yes protein tyrosine kinase from a bacterial expression system. *Arch. Biochem. Biophys.* **1997**, *345*, 135−142.
(10) Sun, G.; Budde, R. J. Substitution studies of the second divalent metal cation requirement of protein tyrosine kinase CSK. *Biochemistry* **1999**, *38*, 5659−5665.
(11) Budde, R. J. A.; Ramdas, L.; Sun, G. Cloning, expression, purification and characterization of the alternate splice Src variants for drug discovery. *J. Mol. Catal.* **2001**, *11*, 805−809.
(12) Saylor, P.; Wang, C.; Hirai, T. J.; Adams, J. A. A second magnesium ion is critical for ATP binding in the kinase domain of the oncoprotein v-Fps. *Biochemistry* **1998**, *37*, 12624−12630.
(13) Vicario, P. P.; Saperstein, R.; Bennun, A. Role of divalent metals in the kinetic mechanism of insulin receptor tyrosine kinase. *Arch. Biochem. Biophys.* **1988**, *261*, 336−345.
(14) Koland, J. G.; Cerione, R. A. Activation of the EGF receptor tyrosine kinase by divalent metal ions: comparison of holoreceptor and isolated kinase domain properties. *Biochim. Biophys. Acta.* **1990**, *1052*, 489−498.
(15) Hubbard, S. R. Crystal structure of the activated insulin receptor tyrosine kinase in complex with peptide substrate and ATP analog. *EMBO J.* **1997**, *16*, 5572−5581.
(16) Adams, J. A.; Taylor, S. S. Divalent metal ions influence catalysis and active-site accessibility in the cAMP-dependent protein kinase. *Protein Sci.* **1993**, *2*, 2177−2186.
(17) Sun, G.; Budde, R. J. Affinity purification of Csk protein tyrosine kinase based on its catalytic requirement for divalent metal cations. *Protein Expression Purif.* **2001**, *21*, 8−12.
(18) Kim, D. H.; Mobashery, S. Mechanism-based inhibition of zinc proteases. *Curr. Med. Chem.* **2001**, *8*, 959−865.
(19) Cohen, S. M.; Lippard, S. J. Cisplatin: from DNA damage to cancer chemotherapy. *Prog. Nucleic Acid Res. Mol. Biol.* **2001**, *67*, 93−130.
(20) Farrell, N. Current status of structure−activity relationships of platinum anticancer drugs: activation of the trans geometry. *Met. Ions Biol. Syst.* **1996**, *32*, 603−639.
(21) Janc, J. W.; Clark, J. M.; Warne, R. L.; Elrod, K. C.; Katz, B. A.; Moore, W. R. A novel approach to serine protease inhibition: kinetic characterization of inhibitors whose potencies and selectivities are dramatically enhanced by zinc(II). *Biochemistry* **2000**, *39*, 4792−4800.
(22) Katz, B. A.; Clark, J. M.; Finer-Moore, J. S.; Jenkins, T. E.; Johnson, C. R.; Ross, M. J.; Luong, C.; Moore, W. R.; Stroud, R. M. Design of potent selective zinc-mediated serine protease inhibitors. *Nature* **1998**, *391*, 608−612.
(23) Katz, B. A.; Luong, C. Recruiting Zn^{2+} to mediate potent, specific inhibition of serine proteases. *J. Mol. Biol.* **1999**, *292*, 669−684.
(24) Rao, M. J.; Sethuram, B.; Rao, T. N. Synthesis and spectroscopic and fungicidal characterization of hydroxamic acids and their metal chelates. *J. Inorg. Biochem.* **1985**, *24*, 155−160.
(25) Farkas, E.; Kovacs, A. Hydroxamic acid derivatives of phenylalanine, tyrosine and 3,4-dihydroxyphenylalanine (DOPA) as ligands. *J. Coord. Chem.* **1991**, *24*, 325−332.
(26) Chang, C. A.; Sekhar, V. C.; Garg, B. S.; Guziec, F. S., Jr.; Carrera Russo, T. Equilibria and kinetics of some metal complexes of peptide hydroxamic acids. *Inorg. Chim. Acta* **1987**, *135*, 11−18.
(27) Li, J.-Z.; Zhang, C.-C.; Zhou, B.; Qin, S.-Y. Synthesis of cobalt(II) complexes with *p-tert*-butylcalix[4]arene-supported dihydroxamic acids. *J. Chem. Res.* **2004**, *9*, 624−625.
(28) Abu-Dari, K.; Raymond, K. N. Coordination isomers of biological iron transport compounds. 8. The resolution of tris(hydroxamato) and tris(thiohydroxamato) complexes of high-spin iron(III). *J. Am. Chem. Soc.* **1977**, *99*, 2003−2005.
(29) Nagata, K.; Mizukami, S. Studies on thiohydroxamic acids and their metal chelates. IV. Reaction of thiohydroxamic acids with metal ions. *Chem. Pharm. Bull.* **1967**, *15*, 61−69.
(30) Abu-Dari, K.; Cooper, S. R.; Raymond, K. N. Coordination chemistry of microbial iron transport compounds. 15. Electrochemistry and magnetic susceptibility of iron(III)-hydroxamate and -thiohydroxamate complexes. *Inorg. Chem.* **1978**, *17*, 3394−3397.

JM061058C